Nano-Micro Lett. (2016) 8(2):143–150
DOI 10.1007/s40820-015-0069-x

ARTICLE

A Hybrid Electrode of Co_3O_4@PPy Core/Shell Nanosheet Arrays for High-Performance Supercapacitors

Xiaojun Yang[1] · Kaibing Xu[1] · Rujia Zou[1] · Junqing Hu[1]

Received: 17 August 2015 / Accepted: 14 September 2015 / Published online: 15 October 2015

Abstract Herein, combining solverthermal route and electrodeposition, we grew unique hybrid nanosheet arrays consisting of Co_3O_4 nanosheet as a core, PPy as a shell. Benefiting from the PPy as conducting polymer improving an electron transport rate as well as synergistic effects from such a core/shell structure, a hybrid electrode made of the Co_3O_4@PPy core/shell nanosheet arrays exhibits a large areal capacitance of 2.11 F cm^{-2} at the current density of 2 mA cm^{-2}, a ~4-fold enhancement compared with the pristine Co_3O_4 electrode; furthermore, this hybrid electrode also displays good rate capability (~65 % retention of the initial capacitance from 2 to 20 mA cm^{-2}) and superior cycling performance (~85.5 % capacitance retention after 5000 cycles). In addition, the equivalent series resistance value of the Co_3O_4@PPy hybrid electrode (0.238 Ω) is significantly lower than that of the pristine Co_3O_4 electrode (0.319 Ω). These results imply that the Co_3O_4@PPy hybrid composites have a potential for fabricating next-generation energy storage and conversion devices.

Keywords Co_3O_4@PPy · Core/shell nanosheet arrays · Supercapacitors

1 Introduction

With the rapid increasing demand in energy storage system for portable electronics and hybrid electric vehicles, supercapacitors have aroused widespread research interest owning to their high power density, fast charge–discharge rate and long lifespan [1–3]. As for a key component of the supercapacitors, electrode materials can be divided into three major types: carbon materials [4, 5], transition metal oxides [6–8] and conducting polymers (CPs) [9, 10]. Carbon materials store charges electrostatically through reversible ion adsorption at the electrode/electrolyte interface [11]. In comparison, transition metal oxides and CPs exploit the fast and reversible Faradic redox process at the electrode surface, thus delivering a considerably high specific capacitance [12, 13]. Therefore, the electrode materials based on transition metal oxides and CPs are gradually becoming a research hotspot in the field of the supercapacitors [14–16].

Among various electrode materials, Co_3O_4 is one of the most extensively investigated pseudocapacitive materials because of its low cost, environmental friendliness and high theoretical capacitance (~3560 F g^{-1}) [8]. Importantly, it can provide multiple oxide states for reversible redox process [17]. Despite these appealing features, the real specific capacitance obtained from various Co_3O_4 nanostructures [18–20] is still far below the theoretical value, which may be attributed to its intrinsic semiconducting characteristic [21]. To overcome this problem, one effective method is

Electronic supplementary material The online version of this article (doi:10.1007/s40820-015-0069-x) contains supplementary material, which is available to authorized users.

✉ Rujia Zou
rjzou@dhu.edu.cn

✉ Junqing Hu
hu.junqing@dhu.edu.cn

[1] State Key Laboratory for Modification of Chemical Fibers and Polymer Materials, College of Materials Science and Engineering, Donghua University, Shanghai 201620, People's Republic of China

fabricating addictive/binder-free electrode configuration to avoid the "dead surface" and tedious process in traditional slurry-coating electrode. Ni foam is widely used as the substrate to support metal oxides materials because of its good electrical conductivity and porous structure, which can enhance the electron transport and improve the active site of electrode materials. Simultaneously, another feasible method is designing three-dimensional (3D) hybrid electrode with large surface area and fast electron transport. Recently, integrating carbon materials, CPs, or noble metal nanoparticles onto electroactive materials has been demonstrated to be an effective synthesis route. Wang et al. [22] successfully prepared Co_3O_4@MWCNTs hybrid composites, which show superior electrochemical performance as positive electrode materials. As one of the most important CPs, polypyrrole (PPy) has been a promising pseudocapacitive electrode material because of its low cost, good electrical conductivity, relatively high capacitance, and outstanding mechanical flexibility [23]. For instance, Liu et al. [24] fabricated a supercapacitor electrode composed of CoO@PPy hybrid nanowires, which delivers a remarkably large areal capacitance of 4.43 F cm^{-2} at 1 mA cm^{-2}, excellent rate capability and cycling performance; Hong et al. [25] developed a Co_3O_4@Au-PPy core/shell nanowires electrode, which exhibits a high specific capacitance of 2062 F g^{-1} (6.39 F cm^{-2}) at 5 mA cm^{-2}, with ~68 % retention of the initial capacitance from 5 to 50 mA cm^{-2}. However, Au as a noble metal is quite costly, and the in situ interfacial polymerization process is time-consuming. In contrast, electrodeposition technique has great advantages, such as convenient, low cost, controllable, and efficient. Thus, it is of great interest to develop a low cost and efficient route to fabricate 3D Co_3O_4@PPy hybrid electrode with enhanced electrical conductivity and excellent electrochemical performance for supercapacitor applications.

Based on above consideration, we designed a 3D core/shell nanostructure of uniform PPy thin layer on mesoporous Co_3O_4 nanosheet arrays as a hybrid electrode material through a solvothermal and electrodeposition process. A hybrid electrode made of as-grown Co_3O_4@PPy core/shell nanosheet arrays exhibits a large areal capacitance of 2.11 F cm^{-2} at the current density of 2 mA cm^{-2}, which is superior to 0.54 F cm^{-2} of the pristine Co_3O_4 electrode. Meanwhile, this electrode also displays a good rate capability (1.37 F cm^{-2} at the current density of 20 mA cm^{-2}). Most importantly, the Co_3O_4@PPy hybrid electrode demonstrates a superior cycling performance (~85.5 % capacitance retention after 5000 cycles). Furthermore, the equivalent series resistance (ESR) value of the Co_3O_4@PPy hybrid electrode (0.238 Ω) is significantly lower than that of the pristine Co_3O_4 electrode (0.319 Ω), indicting the enhanced electrical conductivtity.

2 Experimental

2.1 Synthesis of Mesoporous Co_3O_4 Nanosheet Arrays

All reagents used in the work were of analytical grade. A hybrid electrode configuration was prepared by a facile two-step method, which can be easily scaled up. Typically, a piece of Ni foam (ca. 4 × 1 cm^2) was carefully pretreated with 3 M HCl aqueous by ultrasonication for 30 min, and then cleaned with deionized water and absolute ethanol for several times. 2 mmol of $Co(NO_3)_2{\cdot}6H_2O$ and 5 mmol of hexamethylenetetramine (HMT) were dissolved in 25 mL of deionized water and 25 mL of absolute ethanol under magnetic stirring for 30 min. Then, the resulting solution was transferred into a 60 mL Teflon-lined autoclave and a piece of cleaned Ni foam substrate was immersed into it. Subsequently, the autoclave was sealed and maintained in an electric oven at 90 °C for 8 h. After cooling down to room temperature naturally, the products were rinsed with deionized water and absolute ethanol for several times, and then dried at 60 °C for 2 h. Finally, the as-prepared samples were calcined at 300 °C in air for 2 h.

2.2 Synthesis of Co_3O_4@PPy Core/Shell Nanosheet Arrays

PPy thin layer was grown on the surface of mesoporous Co_3O_4 nanosheet arrays by electrodeposition. The procedure of eletrodeposition was accomplished in a three-electrode system by using the Ni foam-supported as-grown Co_3O_4 electrode materials as the working electrode, a Pt foil as the counter electrode, and Ag/AgCl as the reference electrode. Electrolyte for electrodeposition of PPy was prepared by dissolving 0.4 mL of pyrrole (288 mM) and 0.1491 g of KCl (100 mM) into 20 mL of deionized water. Then, the Co_3O_4@PPy core/shell nanosheet arrays were synthesized at 0.8 V for a different duration of 2, 5, 8, and 10 min. Finally, as-prepared Co_3O_4@PPy hybrid electrode materials were rinsed with deionized water and absolute ethanol for several times, and then dried at 60 °C for 2 h.

2.3 Structure Characterization

As-synthesized products were characterized by D/Max-2550 PC X-ray diffractometer (XRD, Rigaku, Cu-Kα radiation), X-ray photoelectron spectroscopy (XPS, PHI5000VersaProbe), scanning electron microscopy (SEM, HITACHI, S-4800) and transmission electron microscopy (TEM, JEOL, JEM-2100F) equipped with an energy-dispersive X-ray spectrometer (EDX). The Co_3O_4@PPy samples were easily

scraped off from the Ni foam substrate for the Fourier transform infrared (FTIR) test, and the FTIR spectrum was recorded on a Nicolet 6700 FTIR spectrometer (Bruker).

2.4 Electrochemical Characterization

Electrochemical measurements were performed on an Autolab electrochemical workstation (PGSTAT302N) using a three-electrode system and 1 M KOH as the electrolyte. A Pt foil and a saturated calomel electrode (SCE) were used as the counter electrode and the reference electrode, respectively. The Ni foam-supported Co_3O_4@PPy and Co_3O_4 electrode materials (ca. 1 cm^2 area) acted directly as the working electrode.

3 Results and Discussion

In this study, the Co_3O_4@PPy hybrid nanosheet arrays were synthesized through a solvothermal and electrodeposition process. The synthesis procedure of the hybrid nanosheet arrays is briefly summarized in the accessible two steps as shown in Fig. 1. Firstly, mesoporous Co_3O_4 nanosheet arrays were grown vertically on the Ni foam via a solvothermal and calcination procedure. The 3D Ni foam has been widely employed as an ideal current collector owning to its uniform macropores, large supporting area (Fig. S1), and high electrical conductivity [26]. Secondly, PPy was continually integrated onto the surface of the mesoporous Co_3O_4 nanosheet arrays via a controllable and efficient electrodeposition technique. The detailed synthesis procedure of Co_3O_4@PPy hybrid nanosheet arrays was described in the Experimental section. In our design, the PPy shell not only enhances the electrical conductivity of the overall electrode that can facilitate electronic and ion diffusion and improve the utilization of electrode materials, but also contributes to the total capacitance owning to its synergistic effects. We envisage that such a unique hybrid nanostructured electrode together with abovementioned merits will display excellent electrochemical performance in charge storage.

Different magnification scanning electron microscopy (SEM) images of the pristine Co_3O_4 nanosheets are shown in Fig. 2a–c, respectively. A low-magnification SEM image (Fig. 2a) shows that the Co_3O_4 nanosheets are densely and uniformly grown on each strip of the Ni foam. As observed in higher-magnification SEM images (Fig. 2b, c), the Co_3O_4 nanosheets are interconnected with each other and approximately perpendicular to the Ni foam, forming a highly porous structure with broad open space. A TEM image (Fig. 2d) verifies that numerous mesopores are uniformly distributed throughout the overall surface of an individual Co_3O_4 nanosheet, and the porous size ranges from 2 to 10 nm, suggesting its mostly ultrathin feature. The formation of the mesopores could be related to the removal of water molecules during oxidative transformation of precursor to Co_3O_4 [27]. Such an electrode material with nearly vertical nanosheet arrays and highly porous structure can provide abundant electroactive sites, which is beneficial to charge transport and ion diffusion without the necessity of binder blocks, thereby resulting in improved charge transfer kinetics. A high-resolution TEM (HRTEM) image shown in Fig. 2e demonstrates that as-synthesized Co_3O_4 nanosheets give lattice fringes with interplanar spacings of 0.286 and 0.244 nm, corresponding to the (220) and (311) plane of the cubic Co_3O_4, respectively. The XRD pattern in Fig. 2f reveals the crystal structure and phase purity of as-synthesized Co_3O_4 nanosheets. All the diffraction peaks can be indexed into a pure face-centered cubic phase Co_3O_4 with a lattice constant of $a = 8.08$ Å (JCPDS Card No. 42-1467).

The interconnected mesoporous Co_3O_4 nanosheet arrays can serve as an effective scaffold for loading additional electroactive pseudocapacitive electrode materials. In order to further enhance the electrochemical performance, PPy was chosen as an appropriate coating deposited on the mesoporous Co_3O_4 nanosheet arrays. The morphology and structure of the Co_3O_4@PPy hybrid composites were characterized by SEM and TEM. As shown in Fig. 3a, b, wrinkle-like PPy thin layer densely covers the surface of the Co_3O_4 nanosheets. Notably, the decoration of the PPy coating significantly increases the thickness and surface roughness of the Co_3O_4 nanosheets, whereas the Co_3O_4@PPy hybrid composites well maintain the ordered nanostructure. The TEM image in Fig. 3c clearly illustrates that partial porous structure has been covered by the PPy coating, as compared with the pristine Co_3O_4 nanosheets. Moreover, XPS measurement was employed to prove the

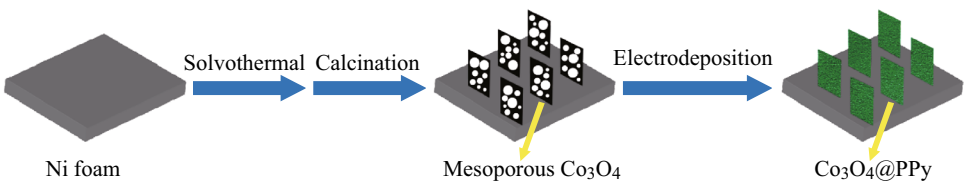

Fig. 1 Schematic diagram for the synthesis of mesoporous Co_3O_4@PPy hybrid nanosheet arrays on Ni foam

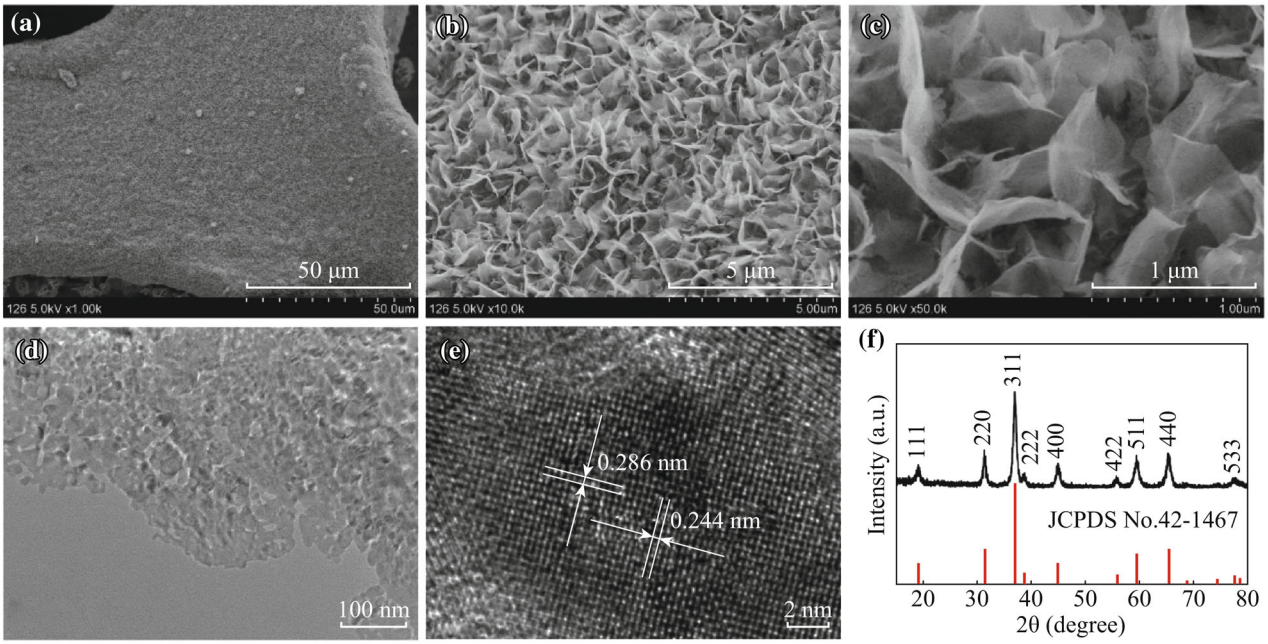

Fig. 2 **a–c** Different magnification SEM images of the mesoporous Co_3O_4 nanosheet arrays on Ni foam. **d**, **e** TEM and HRTEM images of the Co_3O_4 nanosheets. **f** XRD pattern of the Co_3O_4 nanosheets scraped off from the Ni foam

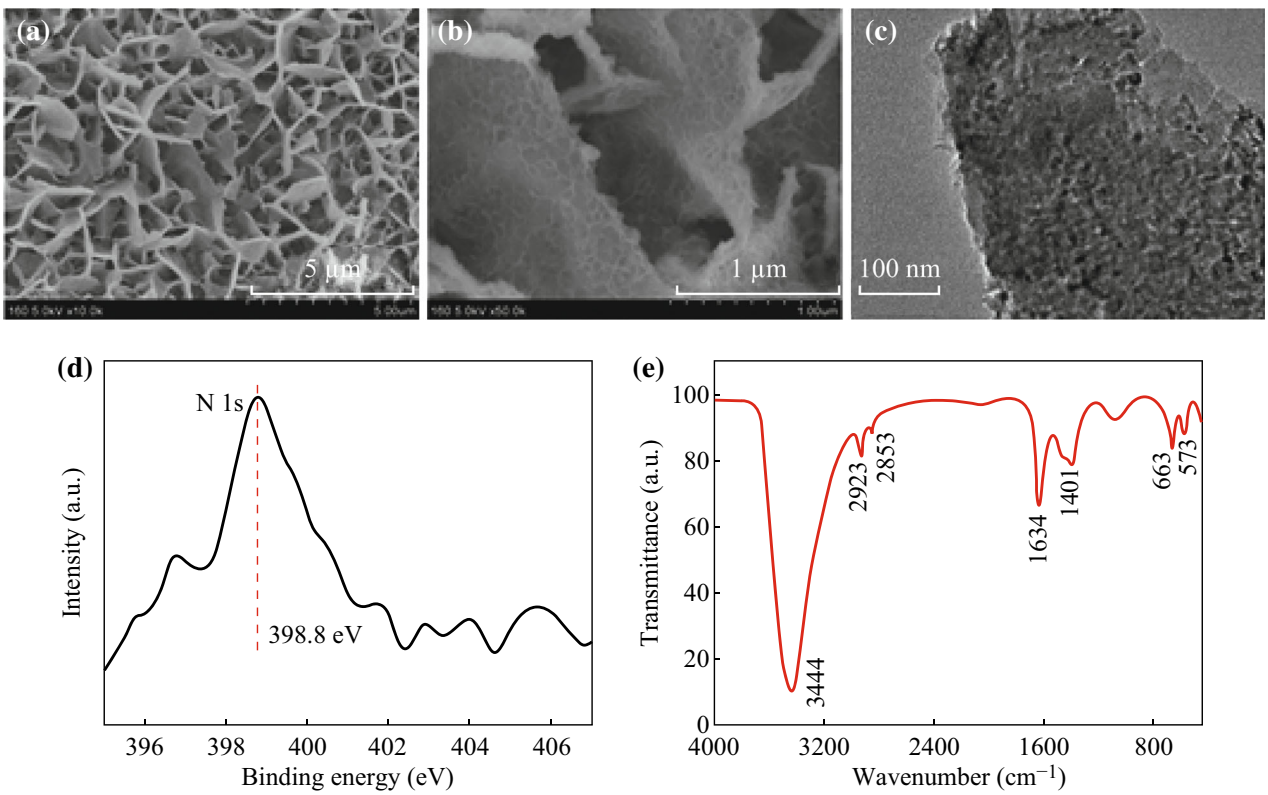

Fig. 3 **a–c** SEM and TEM images of the Co_3O_4@ppy hybrid composites after 5 min electrodeposition. **d** XPS spectrum of N 1 s for the Co_3O_4@ppy hybrid composites. **e** FTIR adsorption spectrum of the Co_3O_4@ppy hybrid composites

existence of the PPy coating. The binding energy of N 1 s peak (Fig. 3d) is centered at 398.8 eV, which corresponds to the neutral nitrogen moieties (–NH–) on PPy [28, 29]. Figure 3e shows the FTIR adsorption spectrum of the Co_3O_4@PPy hybrid composites. A strong adsorption peak at 3444 cm^{-1} should be the stretching vibration of N–H. Two peaks at 1634 and 1401 cm^{-1} are induced by C=C and C–N on the pyrrole ring, respectively [30]. The peaks at 2923 and 2853 cm^{-1} are designated as the asymmetric stretching and symmetric vibrations of CH_2 [31]. Other obvious peaks at 663 and 573 cm^{-1} are attributed to Co–O stretching in Co_3O_4 [32]. According to abovementioned characterizations, we convince that the Co_3O_4@PPy hybrid composites have been successfully synthesized.

To evaluate the electrochemical performance of the Co_3O_4@PPy hybrid electrode using the Co_3O_4 electrode as a comparison, electrochemical measurements were conducted in a three-electrode cell with a Pt counter electrode and a SCE reference electrode in 1 M KOH electrolyte. Figure 4a shows the cyclic voltammetry (CV) curves of the Co_3O_4@PPy hybrid electrode and Co_3O_4 electrode at a scan rate of 50 mV s^{-1} with the potential range of 0 to 0.55 V. It is particularly noteworthy that after coating a PPy thin layer, the enclosed CV curve of the Co_3O_4@PPy hybrid electrode expands drastically, indicating that much larger capacitance is obtained owning to their synergistic effects from two materials of Co_3O_4 and PPy. Firstly, PPy can provide good electrical conductivity, which will definitely result in improved electron transport rate through individual nanosheets. Secondly, PPy itself behaves additional pseudocapacitance during ion doping/dedoping in alkaline solution [24]. Figure 4b displays the CV curves of the Co_3O_4@PPy hybrid electrode at various scan rates. The profile of these curves is not significantly changed with an increasing scan rate from 2 to 80 mV s^{-1}, indicating a reversible electrochemical process and an ideal

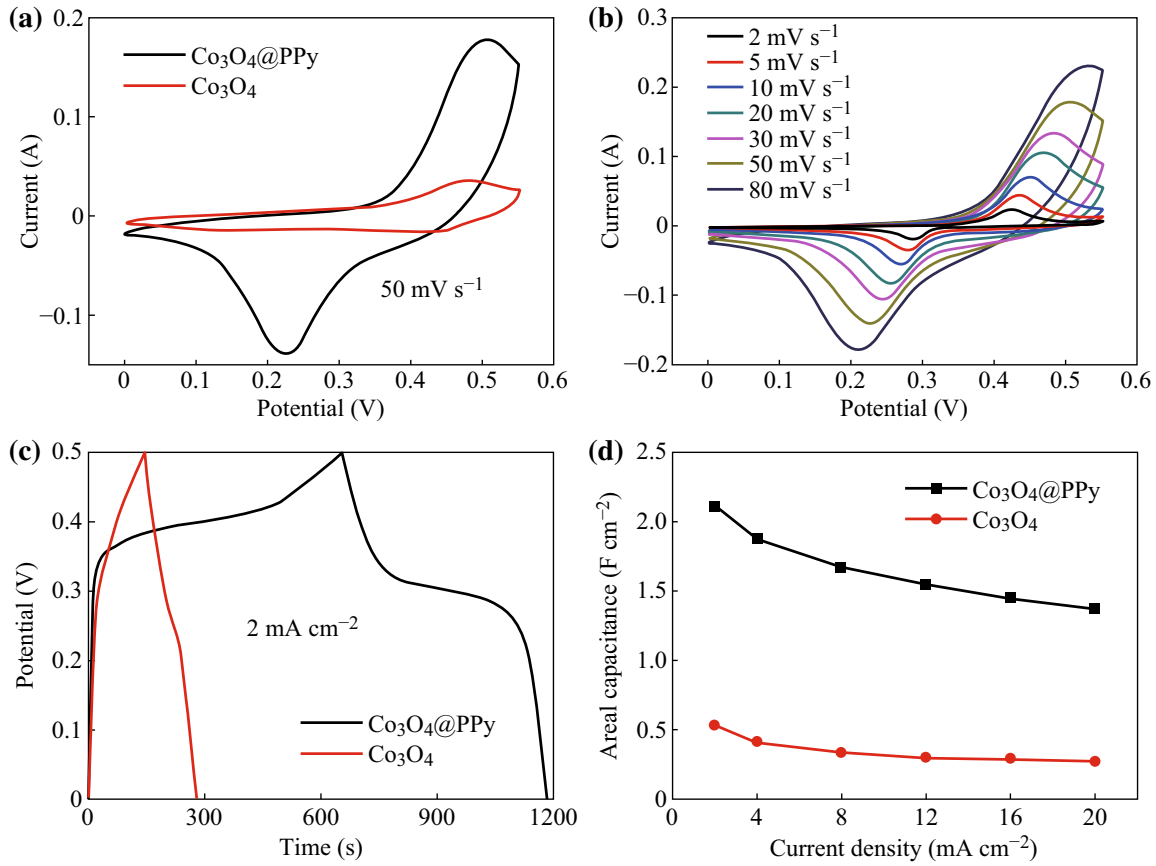

Fig. 4 **a** CV curves of the Co_3O_4@ppy hybrid electrode and Co_3O_4 electrode at a scan rate of 50 mV s^{-1}. **b** CV curves of the Co_3O_4@ppy hybrid electrode and Co_3O_4 electrode at various scan rates. **c** CD curves of the Co_3O_4@ppy hybrid electrode and Co_3O_4 electrode with a current density of 2 mA cm^{-2}. **d** Areal capacitances of the Co_3O_4@ppy hybrid electrode and Co_3O_4 electrode at various current densities

pseudocapacitive characteristic. In addition, the redox peaks slowly move toward positive/negative potential along with the increasing of scan rate, revealing a good contact between the electroactive Co_3O_4@PPy nanosheets and the conductive Ni foam substrate. Figure 4c shows the galvanostatic charge–discharge (CD) curves of the Co_3O_4@PPy hybrid electrode and Co_3O_4 electrode at the current density of 2 mA cm^{-2}. As expected, the Co_3O_4@PPy hybrid electrode displays much longer discharging time than the pristine Co_3O_4 electrode. It denotes that the Co_3O_4@PPy hybrid electrode exhibit much larger areal capacitance than the pristine Co_3O_4 electrode, corresponding to the CV test. The areal capacitances of the Co_3O_4@PPy hybrid electrode and Co_3O_4 electrode are calculated based on the discharge curves (Fig. S2) measured at various current densities via the following formula [33]: $C = I\Delta t/S\Delta V$, where I (A) is the discharge current, Δt (s) is the discharge time, S is the geometric area of the active electrode, and ΔV (V) is the voltage interval, as illustrated in Fig. 4d. Correspondingly, the areal capacitances of the Co_3O_4@PPy hybrid electrode with different electrodeposition times are examined and plotted in Fig. S3. The Co_3O_4@PPy hybrid electrode after 8 min electrodeposition delivers the largest areal capacitance of 2.11 F cm^{-2} at the current density of 2 mA cm^{-2}, which is remarkably larger than the value obtained for the pristine Co_3O_4 electrode (0.54 F cm^{-2}). The Co_3O_4@PPy hybrid electrode still has an areal capacitance of 1.37 F cm^{-2} when the current density is increased to 20 mA cm^{-2}, demonstrating its outstanding rate capability ($\sim$65 %). For comparison, the capacity retention of the pristine Co_3O_4 electrode is only $\sim$50 % at the current density of 20 mA cm^{-2}. To our best knowledge, the excellent electrochemical performance of the Co_3O_4@PPy hybrid electrode presented here is superior to those of previously reported electrodes (see Table 1). Such a large areal capacitance of the as-synthesized Co_3O_4@PPy hybrid electrode will demonstrate a great advantage in improving the energy density of supercapacitors.

Cycling performance is another key factor for supercapacitor applications. Herein, a long-term cycling performance of the as-synthesized electrode materials was examined and compared at a scan rate of 50 mV s^{-1} for 5000 cycles, as shown in Fig. 5a. The overall capacitance retention of the Co_3O_4@PPy hybrid electrode can reach $\sim$85.5 % after 5000 cycles, indicting a superior cycling performance [38–41]; as a comparison, the overall capacitance retention of the pristine Co_3O_4 electrode is 97.7 %, suggesting that the Co_3O_4@PPy hybrid electrode has a $\sim$12 % decrease of the capacitance retention. As is known to all, PPy intrinsically exhibits poor cycling performance caused by its large volumetric swelling and shrinking during ion doping/dedoping process [42]. Therefore, it is not difficult to understand the declining of cycling performance after coating the PPy thin layer. In order to further investigate the electrochemical performance of the as-synthesized electrode materials, electrochemical impedance spectroscopy (EIS) measurement was also conducted to evaluate the electrical conductivity and ion diffusion. As shown in Fig. 5b, the Nyquist plots at higher frequency deliver the ESR value of the Co_3O_4@PPy hybrid electrode (0.238 Ω) and the pristine Co_3O_4 electrode (0.319 Ω), indicating the enhanced electrical conductivity after coating the PPy thin layer [43]. The EIS results imply the easy penetration of the electrolyte into the hybrid electrode and the improved utilization rate of the electrode materials, which can well explain the significantly enhanced areal capacitance as discussed above.

4 Conclusion

In summary, a hybrid nanomaterial of Co_3O_4@PPy core/shell nanosheet arrays on Ni foam was prepared through a solvothermal and electrodeposition process. The Co_3O_4@PPy hybrid electrode exhibits a large areal capacitance of 2.11 F cm^{-2} at the current density of 2 mA cm^{-2}, a $\sim$4-fold enhancement compared with the pristine Co_3O_4 electrode. Furthermore, the Co_3O_4@PPy hybrid electrode also displays good rate capability ($\sim$65 % retention of the initial capacitance from 2 to 20 mA cm^{-2}) and superior cycling performance ($\sim$85.5 % capacitance retention after 5000 cycles). In addition, the ESR value of the Co_3O_4@PPy

Table 1 Comparison of performance metrics for the Co_3O_4@PPy electrode materials with several reported electrode materials in previous literatures

Electrode materials	Areal capacitance	Refs.
Co_3O_4@PPy hybrid composites	2.11 F cm^{-2} at 2 mA cm^{-2}	This work
Mesoporous Co_3O_4 nanosheets	0.54 F cm^{-2} at 2 mA cm^{-2}	This work
Co_3O_4@PPy@MnO_2 core/shell/shell nanowires	1.13 F cm^{-2} at 1.2 mA cm^{-2}	[34]
Co_3O_4@PPy@MnO_2 ternary core/shell composites	0.55 F cm^{-2} at 0.5 A g^{-1}	[35]
Co_3O_4@MnO_2 core/shell nanowires	0.56 F cm^{-2} at 11.25 mA cm^{-2}	[6]
Co_3O_4@NiO core/shell nanowires	1.35 F cm^{-2} at 6 mA cm^{-2}	[12]
ZnO@MnO_2@PPy ternary core/shell nanorods	1.793 F cm^{-2} at 2 A g^{-1}	[36]
FEG/PPy hybrid composites	0.56 F cm^{-2} at 1 mA cm^{-2}	[37]

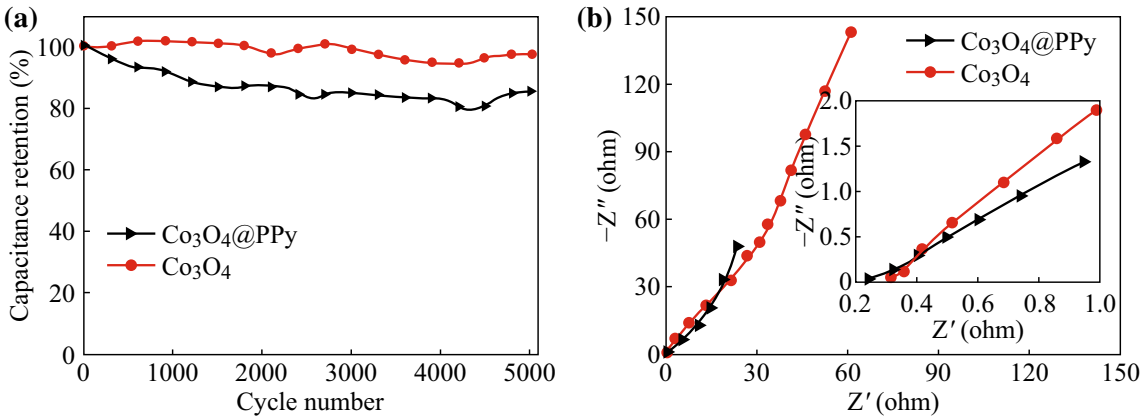

Fig. 5 **a** Cycling performance of the Co_3O_4@ppy hybrid electrode and Co_3O_4 electrode tested at a scan rate of 50 mV s^{-1} for 5000 cycles. **b** Compared EIS curves of the Co_3O_4@ppy hybrid electrode and Co_3O_4 electrode. The *inset* delivers the enlarged nyquist plots at higher frequency

hybrid electrode (0.238 Ω) is significantly lower than that of the pristine Co_3O_4 electrode (0.319 Ω). The outstanding electrochemical performance can enable the Co_3O_4@PPy hybrid composites to be a promising electrode material for next-generation energy storage and conversion devices.

Acknowledgments This work was financially supported by the National Natural Science Foundation of China (Grant No. 21171035, 51472049 and 51302035), the Key Grant Project of Chinese Ministry of Education (Grant No. 313015), the PhD Programs Foundation of the Ministry of Education of China (Grant No. 20110075110008 and 20130075120001), the National 863 Program of China (Grant No. 2013AA031903), the Science and Technology Commission of Shanghai Municipality (Grant No. 13ZR1451200), the Fundamental Research Funds for the Central Universities, the Program Innovative Research Team in University (IRT1221), the Shanghai Leading Academic Discipline Project (Grant No. B603), and the Program of Introducing Talents of Discipline to Universities (No. 111-2-04).

References

1. P. Simon, Y. Gogotsi, Materials for electrochemical capacitors. Nat. Mater. **7**(11), 845–854 (2008). doi:10.1038/nmat2297
2. C. Liu, F. Li, L.P. Ma, H.M. Cheng, Advanced materials for energy storage. Adv. Mater. **22**(8), E28–E62 (2010). doi:10.1002/adma.200903328
3. G.P. Wang, L. Zhang, J.J. Zhang, A review of electrode materials for electrochemical supercapacitors. Chem. Soc. Rev. **41**(2), 797–828 (2012). doi:10.1039/C1CS15060J
4. M. Kaempgen, C.K. Chan, J. Ma, Y. Cui, G. Gruner, Printable thin film supercapacitors using single-walled carbon nanotubes. Nano Lett. **9**(5), 1872–1876 (2009). doi:10.1021/nl8038579
5. Y. Huang, J.J. Liang, Y.S. Chen, An overview of the applications of graphene-based materials in supercapacitors. Small **8**(12), 1805–1834 (2012). doi:10.1002/smll.201102635
6. J.P. Liu, J. Jiang, C.W. Cheng, H.X. Li, J.X. Zhang, H. Gong, H.J. Fan, Co_3O_4 nanowire@MnO_2 ultrathin nanosheet core/shell arrays: a new class of high-performance pseudocapacitive materials. Adv. Mater. **23**(18), 2076–2081 (2011). doi:10.1002/adma.201100058
7. L. Huang, D.C. Chen, Y. Ding, S. Feng, Z.L. Wang, M.L. Liu, Nickel–cobalt hydroxide nanosheets coated on $NiCo_2O_4$ nanowires grown on carbon fiber paper for high-performance pseudocapacitors. Nano Lett. **13**(7), 3135–3139 (2013). doi:10.1021/nl401086t
8. S.J. Peng, L.L. Li, Y.X. Hu, M. Srinivasan, F.Y. Cheng, J. Chen, S. Ramakrishna, Fabrication of spinel one-dimensional architectures by single-spinneret electrospinning for energy storage applications. ACS Nano **9**(2), 1945–1954 (2015). doi:10.1021/nn506851x
9. L. Zheng, Y. Xu, D. Jin, Y. Xie, Polyaniline-intercalated molybdenum oxide nanocomposites: simultaneous synthesis and their enhanced application for supercapacitor. Chem. Asian J. **6**(6), 1505–1514 (2011). doi:10.1002/asia.201000770
10. T.Y. Liu, L. Finn, M.H. Yu, H.Y. Wang, T. Zhai, X.H. Lu, Y.X. Tong, Y. Li, Polyaniline and polypyrrole pseudocapacitor electrodes with excellent cycling stability. Nano Lett. **14**(5), 2522–2527 (2014). doi:10.1021/nl500255v
11. C.G. Liu, Z.N. Yu, D. Neff, A. Zhamu, B.Z. Jang, Graphene-based supercapacitor with an ultrahigh energy density. Nano Lett. **10**(12), 4863–4868 (2010). doi:10.1021/nl102661q
12. X.H. Xia, J.P. Tu, Y.Q. Zhang, X.L. Wang, C.D. Gu, X.B. Zhao, H.J. Fan, High-quality metal oxide core/shell nanowire arrays on conductive substrates for electrochemical energy storage. ACS Nano **6**(6), 5531–5538 (2012). doi:10.1021/nn301454q
13. K. Zhang, L.L. Zhang, X.S. Zhao, J.S. Wu, Graphene/polyaniline nanofiber composites as supercapacitor electrodes. Chem. Mater. **22**(4), 1392–1401 (2010). doi:10.1021/cm902876u
14. X.H. Xia, D.L. Chao, Z.X. Fan, C. Guan, X.H. Cao, H. Zhang, H.J. Fan, A new type of porous graphite foams and their integrated composites with oxide/polymer core/shell nanowires for supercapacitors: structural design, fabrication, and full supercapacitor demonstrations. Nano Lett. **14**(3), 1651–1658 (2014). doi:10.1021/nl5001778
15. F.R. Jiang, W.Y. Li, R.J. Zou, Q. Liu, K.B. Xu, L. An, J.Q. Hu, MoO3/PANI coaxial heterostructure nanobelts by in situ

polymerization for high performance supercapacitors. Nano Energy **7**, 72–79 (2014). doi:10.1016/j.nanoen.2014.04.007
16. H.J. Tang, J.Y. Wang, H.J. Yin, H.J. Zhao, D. Wang, Z.Y. Tang, Growth of polypyrrole ultrathin films on MoS_2 monolayers as high-performance supercapacitor electrodes. Adv. Mater. **27**(6), 1117–1123 (2015). doi:10.1002/adma.201404622
17. C.Z. Yuan, H.B. Wu, Y. Xie, X.W. Lou, Mixed transition-metal oxides: design, synthesis, and energy-related applications. Angew. Chem. Int. Ed. **53**(6), 1488–1504 (2014). doi:10.1002/anie.201303971
18. Y.H. Xiao, S.J. Liu, F. Li, A.Q. Zhang, J.H. Zhao, S.M. Fang, D.Z. Jia, 3D hierarchical Co_3O_4 twin-spheres with an urchin-like structure: large-scale synthesis, multistep-splitting growth, and electrochemical pseudocapacitors. Adv. Funct. Mater. **22**(19), 4052–4059 (2012). doi:10.1002/adfm.201200519
19. R.B. Rakhi, W. Chen, D. Cha, H.N. Alshareef, Substrate dependent self-organization of mesoporous cobalt oxide nanowires with remarkable pseudocapacitance. Nano Lett. **12**(5), 2559–2567 (2012). doi:10.1021/nl300779a
20. C. Feng, J.F. Zhang, Y. He, C. Zhong, W.B. Hu, L. Liu, Y.D. Deng, Sub-3 nm Co_3O_4 nanofilms with enhanced supercapacitor properties. ACS Nano **9**(2), 1730–1739 (2015). doi:10.1021/nn506548d
21. T.Y. Ma, S. Dai, M. Jaroniec, S.Z. Qiao, Metal-organic framework derived hybrid Co_3O_4-carbon porous nanowire arrays as reversible oxygen evolution electrodes. J. Am. Chem. Soc. **136**(39), 13925–13931 (2014). doi:10.1021/ja5082553
22. X.W. Wang, M.X. Li, Z. Chang, Y.F. Wang, B.W. Chen, L.X. Zhang, Y.P. Wu, Orientated Co_3O_4 nanocrystals on MWCNTs as superior battery-type positive electrode material for a hybrid capacitor. J. Electrochem. Soc. **162**(10), A1966–A1971 (2015). doi:10.1149/2.0041511jes
23. G.A. Snook, P. Kao, A.S. Best, Conducting-polymer-based supercapacitor devices and electrodes. J. Power Sources **196**(1), 1–12 (2011). doi:10.1016/j.jpowsour.2010.06.084
24. C. Zhou, Y.W. Zhang, Y.Y. Li, J.P. Liu, Construction of high-capacitance 3D CoO@polypyrrole nanowire array electrode for aqueous asymmetric supercapacitor. Nano Lett. **13**(5), 2078–2085 (2013). doi:10.1021/nl400378j
25. W. Hong, J.Q. Wang, Z.P. Li, S.R. Yang, Hierarchical Co_3O_4@Au-decorated PPy core/shell nanowire arrays: an efficient integration of active materials for energy storage. J. Mater. Chem. A **3**(6), 2535–2540 (2015). doi:10.1039/C4TA04707A
26. G.W. Yang, C.L. Xu, H.L. Li, Electrodeposited nickel hydroxide on nickel foam with ultrahigh capacitance. Chem. Commun. **48**, 6537–6539 (2008). doi:10.1039/b815647f
27. X.H. Xia, J.P. Tu, Y.J. Mai, X.L. Wang, C.D. Gu, X.B. Zhao, Self-supported hydrothermal synthesized hollow Co_3O_4 nanowire arrays with high supercapacitor capacitance. J. Mater. Chem. **21**(25), 9319–9325 (2011). doi:10.1039/c1jm10946d
28. W. Yao, H. Zhou, Y. Lu, Synthesis and property of novel MnO_2@polypyrrole coaxial nanotubes as electrode material for supercapacitors. J. Power Sources **241**, 359–366 (2013). doi:10.1016/j.jpowsour.2013.04.142
29. J. Shao, X.Y. Li, L. Zhang, Q.T. Qu, H.H. Zheng, Core–shell sulfur@polypyrrole composites as high-capacity materials for aqueous rechargeable batteries. Nanoscale **5**(4), 1460–1464 (2013). doi:10.1039/c2nr33590e
30. D.C. Zhang, X. Zhang, Y. Chen, P. Yu, C.H. Wang, Y.W. Ma, Enhanced capacitance and rate capability of graphene/polypyrrole composite as electrode material for supercapacitors. J. Power Sources **196**(14), 5990–5996 (2011). doi:10.1016/j.jpowsour.2011.02.090
31. S. Bose, T. Kuila, M.E. Uddin, N.H. Kim, A.K.T. Lau, J.H. Lee, In-situ synthesis and characterization of electrically conductive polypyrrole/graphene nanocomposites. Polymer **51**(25), 5921–5928 (2010). doi:10.1016/j.polymer.2010.10.014
32. M. Lenglet, J. Lopitaux, L. Terrier, P. Chartier, J. Koenig, E. Nkeng, G. Poillerat, Initial stages of cobalt oxidation by FTIR spectroscopy. J. Phys. IV **03**(C9), 477–483 (1993). doi:10.1051/jp4:1993951
33. G.D. Moon, J.B. Joo, M. Dahl, H. Jung, Y. Yin, Nitridation and layered assembly of hollow TiO_2 shells for electrochemical energy storage. Adv. Funct. Mater. **24**(6), 848–856 (2014). doi:10.1002/adfm.201301718
34. L.J. Han, P.Y. Tang, L. Zhang, Hierarchical Co_3O_4@PPy@MnO_2 core–shell–shell nanowire arrays for enhanced electrochemical energy storage. Nano Energy **7**, 42–51 (2014). doi:10.1016/j.nanoen.2014.04.014
35. B. Wang, X.Y. He, H.P. Li, Q. Liu, J. Wang, L. Yu, H.J. Yan, Z.S. Li, P. Wang, Optimizing the charge transfer process by designing Co_3O_4@PPy@MnO_2 ternary core–shell composite. J. Mater. Chem. A **2**(32), 12968–12973 (2014). doi:10.1039/C4TA02380C
36. W.Q. Ma, Q.Q. Shi, H.H. Nan, Q.Q. Hu, X.T. Zheng, B.Y. Geng, X.J. Zhang, Hierarchical ZnO@MnO_2@PPy ternary core–shell nanorod arrays: an efficient integration of active materials for energy storage. RSC Adv. **5**(50), 39864–39869 (2015). doi:10.1039/C5RA06765K
37. Y. Song, X. Cai, X.X. Xu, X.X. Liu, Integration of nickel–cobalt double hydroxide nanosheets and polypyrrole films with functionalized partially exfoliated graphite for asymmetric supercapacitors with improved rate capability. J. Mater. Chem. A **3**(28), 14712–14720 (2015). doi:10.1039/C5TA02810H
38. W. Tang, L.L. Liu, Y.S. Zhu, H. Sun, Y.P. Wu, K. Zhu, An aqueous rechargeable lithium battery of excellent rate capability based on a nanocomposite of MoO_3 coated with PPy and $LiMn_2O_4$. Energy Environ. Sci. **5**(5), 6909–6913 (2012). doi:10.1039/c2ee21294c
39. Q.T. Qu, Y.S. Zhu, X.W. Gao, Y.P. Wu, Core–shell structure of polypyrrole grown on V_2O_5 nanoribbon as high performance anode material for supercapacitors. Adv. Energy Mater. **2**(8), 950–955 (2012). doi:10.1002/aenm.201200088
40. W. Tang, X.W. Gao, Y.S. Zhu, Y.B. Yue, Y. Shi, Y.P. Wu, K. Zhu, A hybrid of V_2O_5 nanowires and MWCNTs coated with polypyrrole as an anode material for aqueous rechargeable lithium batteries with excellent cycling performance. J. Mater. Chem. **22**(38), 20143–20145 (2012). doi:10.1039/c2jm34563c
41. Y. Liu, B.H. Zhang, S.Y. Xiao, L.L. Liu, Z.B. Wen, Y.P. Wu, A nanocomposite of MoO_3 coated with PPy as an anode material for aqueous sodium rechargeable batteries with excellent electrochemical performance. Electrochim. Acta **116**, 512–517 (2014). doi:10.1016/j.electacta.2013.11.077
42. K. Wang, H.P. Wu, Y.N. Meng, Z.X. Wei, Conducting polymer nanowire arrays for high performance supercapacitors. Small **10**(1), 14–31 (2014). doi:10.1002/smll.201301991
43. X.Y. Liu, S.J. Shi, Q.Q. Xiong, L. Li, Y.J. Zhang, H. Tang, C.D. Gu, X.L. Wang, J.P. Tu, Hierarchical $NiCo_2O_4$@$NiCo_2O_4$ core/shell nanoflake arrays as high-performance supercapacitor materials. ACS Appl. Mater. Interfaces **5**(17), 8790–8795 (2013). doi:10.1021/am402681m